Chinese Chemical Letters 36 (2025) 110201

Contents lists available at ScienceDirect

Chinese Chemical Letters

journal homepage: www.elsevier.com/locate/cclet

Doped cobalt for simultaneously promoting active (001) facet exposure of MIL-68(In) and acting as reactive sites in peroxymonosulfate-mediated photocatalytic decontamination

Chunrui Zhao[a,b], Tianren Li[a,b], Jiage Li[a,b], Yansong Liu[a,b], Zian Fang[a,b], Xinyu Wang[a,b], Mingxin Huo[c], Shuangshi Dong[a,b], Mingyu Li[a,b,*]

[a] Key Laboratory of Groundwater Resources and Environment, Ministry of Education, Jilin University, Changchun 130021, China
[b] Jilin Provincial Key Laboratory of Water Resources and Environment, Jilin University, Changchun 130021, China
[c] Jilin Engineering Laboratory for Water Pollution Control and Resources Recovery, Northeast Normal University, Changchun 130117, China

ARTICLE INFO

Article history:
Received 1 May 2024
Revised 1 June 2024
Accepted 1 July 2024
Available online 1 July 2024

Keywords:
Co doped MIL-68(In)
Exposed facet
PMS/vis system
Peroxymonosulfate activation
Reaction mechanism

ABSTRACT

Rational tuning of crystallographic surface and metal doping were effective to enhance the catalytic performance of metal organic frameworks, but limited work has been explored for achieving modulation of crystal facets and metal doping in a single system. MIL-68(In) was promising for photocatalytic applications due to its low toxicity and excellent photoresponsivity. However, its catalytic activity was constrained by severe carrier recombination and a lack of active sites. Herein, increased (001) facet ratio and active sites exposure were simultaneously realized by cobalt doping in MIL-68(In) through a one-pot solvothermal strategy. Optimized MIL-68(In/Co)-2.5 exhibited remarkable catalytic performance in comparison with pristine MIL-68(In) and other MIL-68(In/Co). The reaction kinetic constant and degradation efficiency of MIL-68(In/Co) were approximately twice and 17% higher than the pristine MIL-68(In) in 36 min reaction, respectively. Density functional theory calculations revealed that Co dopant could modulate the orientation of MIL-68(In) facets, facilitate the exchange of electrons and reduce the adsorption energy of peroxymonosulfate (PMS). This work provides a novel pathway for improvement of In-based MOFs in PMS/vis system, it also promotes the profound comprehension of the correlation between crystal facet regulation and catalytic activation in the PMS/vis system.

The light-driven peroxymonosulfate (PMS)-based advanced oxidation process (AOP) has been regarded as an advanced approach for wastewater treatment owing to its strong oxidization ability and indiscriminate attack of contaminants compared with other treatment strategy. Among the catalysts reported so far, metal organic frameworks (MOFs) as an emerging class of photocatalysts have drawn an increasing attention due to the high specific surface area, controllable porous structure and ease of modification [1–3]. Among them, the MIL-68(In) with abundant indium-oxo clusters possessed high photoresponsivity upon light irradiation for the degradation of antibiotics. However, the light-driven PMS activation of MIL-68(In) was still restrained by low exposure of active sites and the sluggish performance of In [4]. Hence, it is highly important to explore alternative solutions for increasing its reaction sites and catalytic activity.

Recent studies have verified that MOFs with the (001) facet possesses more active sites, and modulating their sufficient exposure will consequently increase the catalytic activity [5]. Various strategies, such as using capping agents, etchants and templating strategies have been applied to regulate the exposure of active facets [6]. However, the above methods might result in uncontrolled reduction in the polymerization of MOFs, leading to the structural damage or collapse [7]. Metal doping was considered as an efficient strategy with the maintenance of the structure [8]. Besides, it can dramatically improve the photoelectric properties by incorporating metal ions into the lattice and further facilitating secondary electron transfer [9].

Cobalt was believed as the optimal active catalysts for PMS activation. However, the reactivity was constrained by the leaching of the cobalt ions during the reaction [10]. It was essential to anchor the cobalt on a suitable carrier to effectively reduce its dissolution. Therefore, we hypothesized that cobalt was anchored on MOFs to continuously catalyze the PMS activation, and to simultaneously achieve the reactive facet exposure.

* Corresponding author.
E-mail address: mingyuli@jlu.edu.cn (M. Li).

https://doi.org/10.1016/j.cclet.2024.110201
1001-8417/

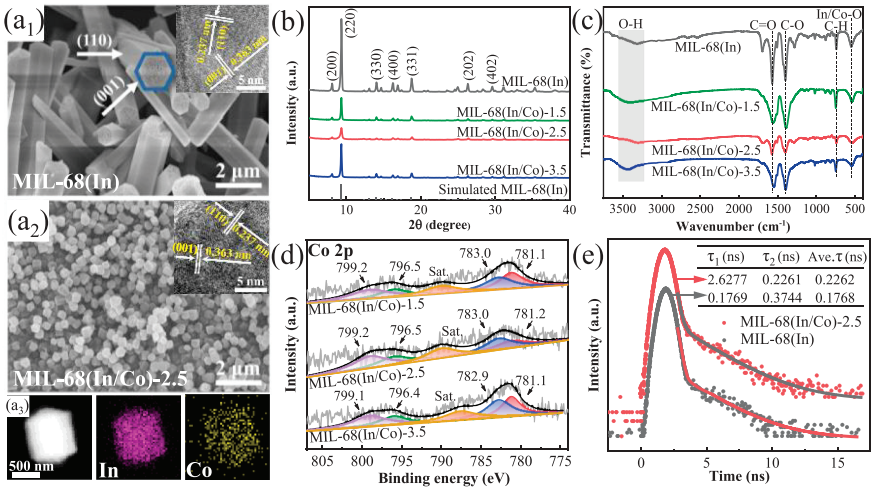

Fig. 1. SEM and TEM images of (a_1) MIL-68(In) and (a_2) MIL-68(In/Co)-2.5, (a_3) HRTEM images of MIL-68(In/Co)-2.5. (b) XRD patterns and (c) FT-IR spectra of MIL-68(In) and MIL-68(In/Co)-X. (d) High-resolution Co 2p XPS spectra of as-prepared catalysts and (e) PL decay curves of MIL-68(In) and MIL-68(In/Co)-2.5.

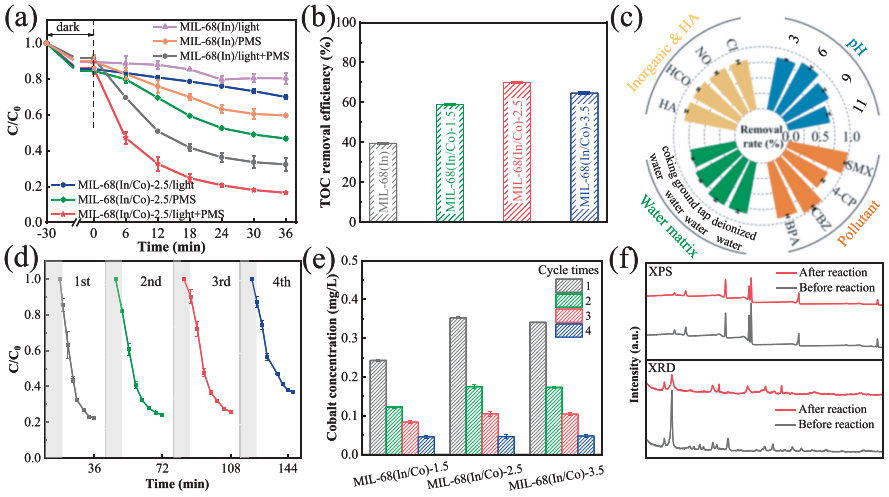

Fig. 2. (a) Degradation performance of catalysts in the PMS/vis system, (b) TOC removal efficiencies, (c) influence of various factors on TCH degradation over MIL-68(In/Co)-2.5. (d) The degradation curves of MIL-68(In/Co)-2.5 in four cycles, (e) leached concentration for cobalt ion of various catalysts and (f) XPS spectra and XRD patterns before and after four cyclic reaction.

Herein, cobalt element was adopted to synthesize a novel Co-doped MIL-68(In) composite to achieve (i) adjusting the exposure ratios of the (001) facet, (ii) understanding the effect of (001) facet exposure ratios on the catalytic performance, and (iii) elucidating the role of (001) facet in PMS adsorption and electron transfer during the PMS activation process.

Scanning electron microscopy (SEM) image (Fig. 1a_1) showed that the MIL-68(In) exhibited typical elongated hexagonal microrods [11]. However, significant decrease to 17.9% of the original length was observed in MIL-68(In/Co)-x (Fig. 1a_2 and Fig. S1 in Supporting information). The introduction of Co inhibited the growth of MIL-68(In) along (001) axial direction [9], possibly because of the formation of thermodynamic barrier resulting from intermolecular interactions and kinetic reactions [12]. The capped facet width and axial length of these hexagonal crystals were *ca.* 0.25–1.0 μm for (001) and 0.4–10.0 μm for (110) facet. The corresponding (001) facet exposure ratio was 38.5% for MIL-68(In/Co)-2.5, which was higher than MIL-68(In) (12.0%), MIL-68(In/Co)-1.5 (32.8%) and MIL-68(In/Co)-3.5 (30.2%) (Table S1 and Text S5 in Supporting information) [13]. This observation suggested that the Co dopant of MIL-68(In/Co)-2.5 resulted in improved facet selective growth.

High-resolution transmission electron microscopy (HRTEM) image of MIL-68(In/Co)-2.5 further demonstrated the existence of (001) and (110) facet with the lattice spacing of *ca.* 0.363 nm and 0.237 nm, respectively (Fig. S2 in Supporting information). Energy dispersive X-ray (EDX) elemental mapping results of MIL-68(In/Co)-2.5 revealed the uniform distribution of In and Co (Fig. 1a_3).

X-ray diffractometer (XRD) patterns of MIL-68(In) and MIL-68(In/Co)-X verified the successful synthesis of MIL-68(In) with a pure crystalline phase (Fig. 1b) [14]. With the increase of cobalt doping ratio, the intensity of the diffraction peaks gradually decreased then increased compared with the pristine MIL-68(In), indicating the variation in the crystallinity of the MOFs. Moreover, the doping of Co did not cause phase changes in the crystals of MIL-68(In), and Co elements might be doped into the lattice of MIL-68(In) [15].

The characteristic peaks presented in Fourier-transform infrared spectroscopy (FT-IR) spectra of all catalysts were found at around

550, 750, 1399, and 1569 cm^{-1} (Fig. 1c), corresponding to the In/Co−O stretching vibration, bending vibration of the C−H bonds in the benzene ring, symmetric and asymmetric vibrations of the O−C=O groups. This indicated the formation of bimetallic centers in the MIL-68(In/Co) framework [16].

X-ray photoelectron spectrometer (XPS) survey spectra of MIL-68(In/Co) presented the C, O, In and Co elements (Fig. S3a in Supporting information). C=C and −COO, In−O, C=O and C−OH bonds were characteristic peaks in MIL-68(In/Co)-2.5, respectively [17,18]. Fig. S3d presented the In 3d spectra with two characteristic peaks centered around 445.0 (In $3d_{5/2}$) and 452.6 eV (In $3d_{3/2}$) [19]. The In 3d peak of MIL-68(In/Co) shifted to a higher binding energy, which was due to the fact that the incorporation of Co changed the electronic structure of In center, resulting in its reduced the electron cloud density [20]. The Co 2p spectra displayed two peaks (Fig. 1d), assigned to $2p_{3/2}$ and $2p_{1/2}$ orbitals of Co^{2+} (781.8 and 796.5 eV) [21]. In contrast, the Co 2p characteristic peak shifted towards a lower binding energy by 0.1–0.2 eV. The observed shift indicated the migration of electron density from In to Co caused by bimetallic interactions after the introduction of Co(II) [22].

The MIL-68(In/Co)-X exhibited a noticeable variation in photocurrent during the switching cycle of light source (Fig. S4a in Supporting information). Notably, the transient photocurrent of MIL-68(In/Co)-2.5 was approximately 3 times higher than that of MIL-68(In), which indicated the photogenerated carriers were effectively separated and the interfacial transport efficiency were improved [23]. The electrochemical impedance spectrum showed that MIL-68(In/Co)-2.5 had the smallest arc radius at the high-frequency region, which was corresponding to the lowest impedance than the other catalysts (Fig. S4b in Supporting information). Therefore, the introduction of Co contributed to a faster photogenerated carrier transfer rate [24]. The UV–vis diffuse reflectance spectra (DRS) of the MIL-68(In/Co) showed stronger absorption intensity in UV–vis region (Fig. S4d in Supporting information). Most importantly, MIL-68(In/Co)-2.5 exhibited stronger absorption intensity in UV–vis region, reflecting the influence of the energy band structure by the exposed crystalline surface ratio [25]. The enhanced light absorption could be attributed to the incorporation of Co doping, which acts as the active site and controls the exposure ratios in the (001) facet [26].

The photoluminescence (PL) spectra in Fig. 1e and Fig. S4c (Supporting information) illustrated that the MIL-68(In/Co)-2.5 exhibited the lowest PL response among all the samples. The time-resolved decay spectroscopy PL illustrated that the average lifetime of MIL-68(In/Co)-2.5 (0.23 ns) was longer than that of MIL-68(In) (0.18 ns), indicating that the carrier recombination of MIL-68(In/Co)-2.5 was suppressed. The extended lifetime was probably due to the optimized radiative decay pathways facilitated by the (001) facets, which effectively reduce nonradiative decay channels [13]. All these observations suggested that the introduced Co dopant with increased percentage of exposed (001) facet can enhance the photogenerated charge generation, separation and transfer, which was beneficial for the modification of photo-PMS activity of MIL-68(In/Co)-2.5.

Tetracycline (TCH), as a typical persistent organic pollutant, was chosen as the model pollutant to evaluate the photocatalytic properties of catalysts in the PMS/vis system and to mitigate its hazards. The photocatalytic performance of MIL-68(In/Co)-X was improved dramatically with the Co doping (Fig. 2a and Fig. S6a in Supporting information). The degradation efficiency decreased in the order of MIL-68(In/Co)-2.5 > MIL-68 (In /Co)-3.5 > MIL-68 (In /Co)-1.5, which was consistent with the exposure ratio of (001) surface for the photocatalysts (Fig. S7 in Supporting information). Therefore, the introduction of cobalt in MIL-68(In) with the modification of the (001) facet exposure ratio and reactive sites led to an enhanced PMS/vis activation performance [16].

The presence of light or PMS alone resulted in negligible TCH removal efficiency for MIL-68(In) and MIL-68(In/Co)-2.5 (Fig. 2a and Fig. S6b in Supporting information). With the addition of MIL-68(In/Co)-2.5, the degradation efficiency in the PMS/vis system (84.0%) was much higher compared to that of PMS (46.1%) or light only (31.0%) due to the synergistic effect [27]. The total organic carbon (TOC) removal by MIL-68(In/Co)-2.5 in the PMS/vis system was as high as ~70% (Fig. 2b), further confirming the superior mineralization activity.

Further optimization of experimental conditions was considered by adjustment of the catalyst and PMS dosage. When the catalyst dosage was less than 150 mg/L, the TCH removal efficiency was improved with increasing dosage (Fig. 2c). However, excessive catalyst constrained the removal efficiency due to an increased turbidity of the water column, reducing the penetration of light [18]. When the PMS dosage was varied from 0.625 mmol/L to 5.0 mmol/L, TCH removal efficiency increased due to the production of more active substances. But PMS decomposition generated SO_4^{2-}, leading to a secondary pollution [28]. Considering saving economic costs and reducing environmental harm, the dosage of catalyst and PMS was determined as 150 mg/L and 2.5 mmol/L.

The effects of pH value, inorganic ions, water matrices and emerging pollutants were further considered for the catalytic activity of MIL-68(In/Co)-2.5. TCH removal performance was highest at pH 6, and strongly acidic or alkaline environments were detrimental to TCH degradation (Fig. 2c). The evolving surface charge of MIL-68(In/Co)-2.5 with various pH was shown in Text S7 and Fig. S8 (Supporting information). The degradation capacity of MIL-68(In/Co)-2.5 was slightly decreased in the water body with various anions (Cl^-, NO_3^- and HCO_3^-) and humic acids (HA), implying that inorganic matter had little effect on degradation of TCH in PMS/vis system. 83.9%, 84.1%, 79.4% and 74.5% of TCH were removed from deionized water, tap water, groundwater and coking wastewater, respectively. High chromaticity, turbidity with phenols and cyanide inhibited TCH removal, leading to a dramatical decrease in degradation efficiency of coking wastewater [29]. MIL-68(In/Co)-2.5 showed high degradation rates of 92.0%, 98.9%, 92.0% and 78.9% for carbamazepine (CBZ) and sulfamethoxazole (SMX), bisphenol A (BPA) and *p*-chlorophenol (4-CP) in 36 min degradation. Moreover, Table S2 (Supporting information) compared the performance of as-prepared MIL-68(In/Co)-2.5 with others reported in literature. The distinguished removal efficiency and reaction rate with lower catalyst concentration and PMS dosage indicated that MIL-68(In/Co)-2.5 is a promising photocatalyst for TCH and other contaminant removals.

The photocatalytic activity of MIL-68(In/Co)-2.5 remained essentially stable in four cyclic experiments (Fig. 2d). The slight decrease in catalyst performance could be attributed to the accumulation of intermediates on the active surface sites of the photocatalysts. XRD patterns, XPS (Fig. 2f and Fig. S9 in Supporting information) and DRS (Fig. S10 in Supporting information) spectra of MIL-68(In/Co)-2.5 showed no noticeable change after four runs. The Co leaching concentration of MIL-68(In/Co)-X after reaction was 0.24 mg/L, 0.35 mg/L and 0.34 mg/L, which were far below the limit (1.0 mg/L) by European Union, and lower compared to the reported literatures (Fig. 2e and Table S2). The trace cobalt ions had negligible effect on the degradation process [30]. These results demonstrated the superior stability of MIL-68(In/Co)-2.5 for TCH removal.

The degradation pathway deduced based on the liquid chromatograph with mass spectrometer (LC-MS) results showed that TCH molecule (*m/z* 445) first underwent dehydration and hydroxylation, resulting in the formation of **P1** (*m/z* 461) (Figs. S11 and S12 in Supporting information). Next, the branched chained on the benzene ring were further removed through demethylation and dehydroxylation, leading to the production of **P2** (*m/z* 410), **P5** (*m/z*

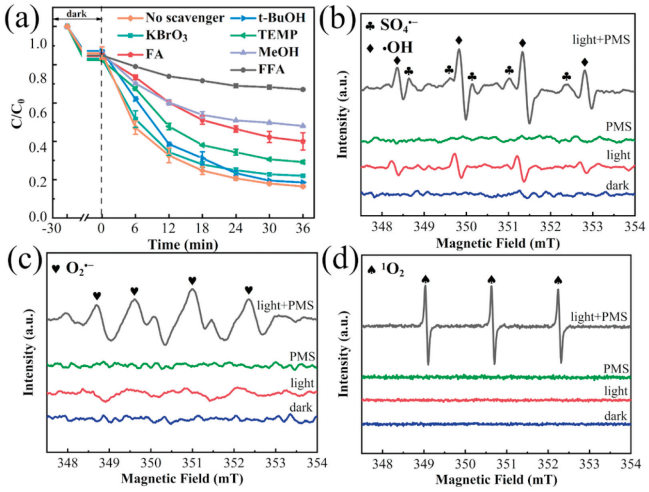

Fig. 3. (a) ROS scavenger experiment with MIL-68(In/Co)-2.5 in PMS/vis system. ESR spectra of (b) $^{\bullet}OH$, $SO_4^{\bullet-}$, (c) $^{\bullet}O_2^-$ and (d) $^1O_2$.

427), **P6** (*m/z* 397), **P7** (*m/z* 296) and **P9** (*m/z* 416) [31]. Afterward, TCH was decarbonylated and deaminated, giving rise to simple aromatic compounds **P3** (*m/z* 366), **P4** (*m/z* 257), **P8** (*m/z* 230) and **P10** (*m/z* 352), which gradually cleaved into smaller organic fragments [32].

The toxicity of TCH and its intermediates was calculated using T.E.S.T. software. The acute toxicity of half intermediates of fathead minnow during degradation was higher than that of TCH, which may be related to the formation of electrophilic groups (Fig. S13 in Supporting information) [33]. For mutagenicity factors, the vast majority of TCH products exhibited positive mutagenicity values. Besides, the intermediates showed diminished developmental toxicity and an elevated trend of bioaccumulation factors. The combined analysis results indicated that MIL-68(In/Co)-2.5 and its corresponding intermediates in catalytic degradation of TCH were mostly environmentally friendly.

Radical capture experiments demonstrated the degradation was significantly inhibited by the addition of furfuryl alcohol (FFA) and methanol (MeOH). Specifically, the presence of FFA resulted in a reduction of the degradation efficiency by 50.6%. Therefore, $^1O_2$ species were identified as the primary active species for promoting the degradation of TCH, and $SO_4^{\bullet-}$ played a secondary role (Fig. 3a). Electron spin resonance spectra (ESR) measurements were further used to confirm the types of ROS. No signal was detected in dark, while a faint signal was observed under light. However, the system with light and PMS involvement exhibited strong $SO_4^{\bullet-}$ and $^{\bullet}OH$ signals, suggesting that MIL-68(In/Co)-2.5 can indeed activate PMS to produce both radicals (Fig. 3b). $^1O_2$ and $^{\bullet}O_2^-$ were verified similarly and the intensity of the signal followed the same rule (Figs. 3c and d). The ESR results agreed with those obtained from the quenching experiments.

Figs. 4a and b showed the optimized structures of PMS adsorption on (001) and (110) facets of different catalysts. $HSO_5^{\bullet-}$ (PMS) adsorption energies (E_{ads}) for MIL-68(In)−001 and MIL-68(In/Co)-001 were found lower in comparison to MIL-68(In)−110 and MIL-68(In/Co)-110. This observation strongly supported the hypothesis that the (001) facet of MIL-68(In/Co) exhibited higher efficiency in terms of PMS adsorption and activation [34]. The results showed that the (001) facets with Co modified MIL-68(In) had a significantly enhanced affinity to adsorb PMS over the (110) facets, which was beneficial for PMS activation and consistent with the degradation results. Co doping might alter the crystal structure and electronic state of MIL-68(In) and further affect its interaction with PMS.

Differential charge densities of MIL-68(In)−001 demonstrated lower electron density around benzene ring than that of PMS, and Co dopant further led to the electron deficiency around In (Figs. S14a and b in Supporting information). The results indicated that the charge underwent rearrangement and promoted TCH removal. The inter-element interactions were then probed by in-depth analysis of the density of states (DOS) of the catalyst. The VB top consisted of In 3d and O 2p orbitals, while the CB bottom consisted mainly of C 1s orbitals. The MIL-68(In/Co)-001 overlapped between In and Co orbitals near the zero point and showed small waves, representing their strong interaction (Fig. 4c) [35]. Besides, MIL-68(In/Co)-001 had a broader and lower overall peak compared to MIL-68(In)−001, which represented the high off-domain energy. Additionally, the Co peak of MIL-68(In/Co)-001 near the Fermi energy level was at the uppermost, which means that the excited state electrons jump to the impurity energy level through the empty orbitals of cobalt. Fig. 4d showed that the larger energy gap in the DOS diagram of MIL-68(In/Co)-110 compared to MIL-68(In/Co)-001, which suggested the need of higher energy to excite electrons. Additionally, MIL-68(In/Co)-110 exhibited fewer flat regions in the electronic density of states curve, indicating a lower electron density at specific energy levels and a relatively low utilization of electronic energy levels. The band gap showed in Figs. S15a-d (Supporting information). It was worth noting that both the (001) facets dominant and Co doped MIL-68(In/Co) had much narrower band gaps compared to (110) facets dominant MIL-68(In/Co) and original MIL-68(In), which was conductive to photoexcitation.

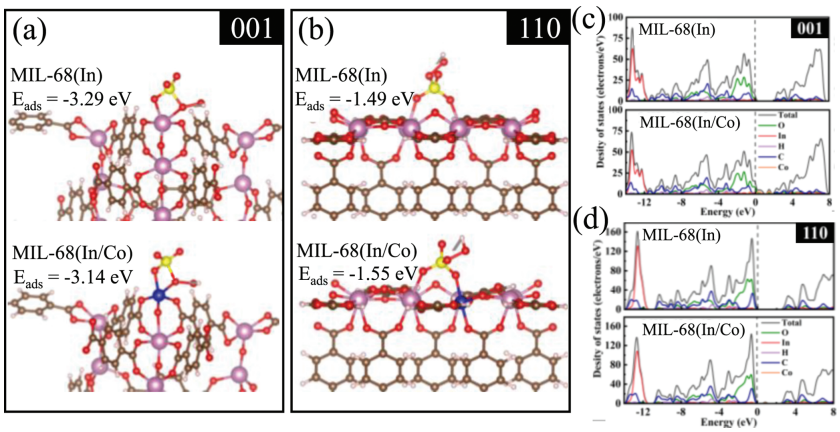

Fig. 4. (a, b) DFT calculation of $HSO_5^{\bullet-}$ (PMS) adsorption and (c, d) density of states on various catalysts with different crystal plane. The pink, blue, yellow, red and brown balls are In, Co, S, O and C atoms.

A potential photocatalytic reaction mechanism for the degradation of TCH using MIL-68(In/Co)-2.5 could be proposed. The hexagonal crystal MIL-68(In/Co)-2.5 was stimulated by light, leading to the generation of electron-hole pairs [36]. The electron transferred to the surface of MIL-68(In/Co)-2.5 induced the cleavage of the peroxide bond (−O−O−) in PMS by Co^{2+} through single electron transfer to produce $SO_4^{\bullet-}$ and $^{\bullet}OH$. At the same time, Co^{3+} was converted to Co^{2+} by reduction reaction with PMS to produce $SO_5^{\bullet-}$ [37]. The reaction between the photogenerated e^- and oxygen resulted in the production of $^{\bullet}O_2^-$. Next, $SO_5^{\bullet-}$ reacted with H_2O to produce $^1O_2$. In addition, PMS might be self-decomposed to produce the paired radicals $SO_5^{\bullet-}$, which further convert to $S_2O_8^{2-}$ and $^1O_2$. Finally, the resulting $SO_4^{\bullet-}$ and $^1O_2$ completed the degradation of TCH by addition and deamination reactions, respectively [38].

In summary, bimetallic MIL-68(In/Co) with (001) facet exposure was constructed by a one-pot solvothermal strategy. The exposed ratios of (001) in MIL-68(In/Co) were finely tailored by varying the Co content during the synthetic reaction. When fully exposed to the (001) facet, MIL-68(In/Co)-2.5 exhibited superior activation ability in the generation of ROS under light irradiation. Notably, the inclusion of Co dopant facilitated the transfer of electrons and decreased the adsorption energy of PMS by (001) facet. Furthermore, the interaction between the In/Co bimetallic sites accelerated the PMS activation, which promoted the formation of the $^1O_2$ and $SO_4^{\bullet-}$. The work not only provided new insights into design and development of highly effective photocatalysts through facet engineering, but also offered an efficient and stable bimetallic catalyst for wastewater treatment. The exploration for the reduction of the cost is on the way.

Declaration of competing interests

The authors declare that they have no known competing financial interests or personal relationships that could have appeared to influence the work reported in this paper.

Acknowledgments

This work was financially supported by the National Natural Science Foundation of China (Nos. 52100087, 52170079, U20A20322), Science and Technology Development Program of Jilin Province, China (Nos. 20220508100RC, 20230402035GH).

Supplementary materials

Supplementary material associated with this article can be found, in the online version, at doi:10.1016/j.cclet.2024.110201.

References

[1] S. Ma, Z. Zhou, Y. Zhang, et al., Sep. Purif. Technol. 339 (2024) 126636.
[2] N. Liu, D. Wang, J. Xu, et al., Surf. Interfaces 46 (2024) 104192.
[3] J. Wei, Y. Zhang, Z. Zhou, et al., Prog. Nat. Sci. 33 (2023) 872–880.
[4] J. Panda, S.P. Tripathy, S. Dash, et al., Nanoscale 15 (2023) 7640–7675.
[5] F. Wang, Z. Yang, Z. Yang, et al., Chem. Eng. J. 450 (2022) 138166.
[6] S. Bai, L. Wang, Z. Li, et al., Adv. Sci. 4 (2017) 1600216.
[7] S. Sun, L. He, M. Yang, et al., Adv. Funct. Mater. 32 (2022) 2106982.
[8] Y. Zhang, H. Guo, J. Ren, et al., Appl. Catal. B: Environ. 298 (2021) 120582.
[9] T. Zhong, Z. Yu, R. Jiang, et al., Sol. RRL 5 (2021) 2100223.
[10] D. Liu, Z. Su, B. Han, et al., Appl. Catal. B: Environ. 330 (2023) 122555.
[11] J. Li, L. Liu, Q. Liang, et al., J. Hazard. Mater. 414 (2021) 125395.
[12] A. Amine-Khodja, A. Boulkamh, C. Richard, Appl. Catal. B: Environ. 59 (2005) 147–154.
[13] H. Zhao, X. Liu, Y. Dong, et al., ACS Appl. Mater. Inter. 12 (2020) 31532–31541.
[14] H. Song, Q. Zhang, D. Hu, Z. Sun, et al., Sep. Purif. Technol. 287 (2022) 120585.
[15] L. Kumaresan, A. Prabhu, M. Palanichamy, et al., J. Hazard. Mater. 186 (2021) 1183–1192.
[16] H. Liang, R. Liu, C. Hu, et al., J. Hazard. Mater. 406 (2020) 124692.
[17] S. He, Z. Li, J. Wang, J. Solid. State. Chem. 307 (2022) 122726.
[18] J. Wei, Q. Wang, M. He, et al., Appl. Surf. Sci. 612 (2023) 155726.
[19] S. Wang, B.Y. Guan, X.W.D. Lou, J. Am. Chem. Soc. 140 (2018) 15145–15148.
[20] X. Zhao, B. Pattengale, D. Fan, et al., ACS. Energy. Lett. 3 (2018) 2520–2526.
[21] S.W. Lv, J.M. Liu, N. Zhao, et al., J. Hazard. Mater. 3871 (2023) 122011.
[22] M. Sanad, A. Puente Santiago, S. Tolba, et al., J. Am. Chem. Soc. 143 (2021) 4064–4073.
[23] L. Jiang, X. Yuan, G. Zeng, et al., Appl. Catal. B: Environ. 221 (2018) 715–725.
[24] J. Cao, Z. hui Yang, W. ping Xiong, et al., Chem. Eng. J. 353 (2018) 126–137.
[25] X. Ma, H. Cheng, Chem. Eng. J. 429 (2022) 132373.
[26] J. Li, X. Li, Z. Yin, et al., ACS. Appl. Mater. Interfaces. 11 (2019) 29004–29013.
[27] P. Sarkar, S. Neogi, S. De, J. Hazard. Mater. 451 (2023) 131102.
[28] C. Zhao, B. Shao, M. Yan, et al., Chem. Eng. J. 416 (2021) 128829.
[29] S. Wang, W. An, J. Lu, et al., Chem. Eng. J. 441 (2022) 135944.
[30] H. Wang, S. Yu, X. Meng, et al., J. Solid. State. Chem. 314 (2022) 123431.
[31] L. Xie, Z. Yang, W. Xiong, et al., Appl. Surf. Sci. 465 (2019) 103–115.
[32] X. Wang, Y. Ma, J. Jiang, et al., J. Hazard. Mater. 434 (2022) 128864.
[33] X. Chen, L. Yao, J. He, et al., J. Hazard. Mater. 449 (2023) 131024.
[34] Y. Yang, W. Gong, X. Li, et al., J. Hazard. Mater. 436 (2022) 129246.
[35] X. Wang, C. Zhang, D. Li, et al., J. Hazard. Mater. 454 (2023) 131469.
[36] C. Li, Z. Zhao, X. Wang, et al., Chem. Eng. J. 442 (2022) 136249.
[37] Y. Liu, R. Luo, Y. Li, et al., Chem. Eng. J. 347 (2018) 731–740.
[38] X. Li, T. Hou, L. Yan, et al., J. Hazard. Mater. 398 (2020) 122884.